Solar Heat Recovery from Windows in Light-Frame Wood Construction

G.E. Hans **P. Calthorpe**

ABSTRACT

Changes in thermal performance standards show growing emphasis on the need for heat-gain management in solar building designs having lightweight envelopes. This study investigated one option for such management in light-frame wood construction. Conclusions are drawn from observed field performance of two similar structures of comparable thermal mass; in one of them, solar heat recovered from a collector window was delivered to primary storage by forced airflow rather than by natural convection or radiation. Performance was judged on the basis of heat balance calculations for a 5-day midwinter period. The analytical procedure used excluded solar heat gains that led to unacceptable room temperature swings and could, therefore, no longer be considered useful. A concrete floor slab and rock bed assembly served as the primary heat storage system in both structures. During the collection cycle, the direct-gain structure showed appreciable heat flow from the floor slab to the rock bed and marked temperature differences between mass located directly in the sun and out of the sun. The resulting overheating problems were attributed to a poor load-to-storage coupling rather than to a lack of storage capacity. In the window-heat-recovery structure, the under-floor storage was engaged more effectively; i.e., room temperatures were within an acceptable range and useful solar-gain collection capacity was markedly improved. These observations suggest that window heat recovery may be an effective option for improving solar performance of light-frame wood structures, or of any other construction system offering only limited heat storage capacity in the building envelope.

INTRODUCTION

Current trends in thermal-performance standards for residential buildings show growing emphasis on the management of solar heat gain.[1] The primary solar gain control strategy in basic passive solar design has been to proportion window areas and heat-storage capacity for the desired room temperature control under design conditions.[2] Such design, however, limits versatility in solar-gain management at other-than-design conditions. It also requires the addition of substantial thermal mass to buildings with lightweight envelopes, including typical light-frame wood construction. Mechanically assisted heat transfer, on the other hand, allows more flexible temperature control. One such design option is known as "window heat recovery."[3]

Field performance of window-heat-recovery designs is relatively unexplored. The purpose of this study, therefore, was to test the applicability of the window heat recovery concept to light-frame wood construction. This was done by comparing the solar performance of two similar buildings, one representative of common passive solar design adaptations to wood

---

Architect, Forest Products Laboratory, Forest Service, U.S. Department of Agriculture, in cooperation with the University of Wisconsin, Madison, Wis.

Architect with Van der Ryn, Calthorpe and Partners, and, at the time of the study, Director of Farallones Institute for Solar Design and Research, Occidental, California.

The field research discussed in this report was conducted by the Farallones Institute in northern California. Results of that study have been published by Peter Calthorpe in another report.[13] Any differences that may exist between these two reports are attributable to differences in data processing and judgment of the primary author.

construction and the other based on application of window-heat-recovery concepts to the same architectural design.

Performance was evaluated on the basis of temperature measurements, considered to be the most meaningful reference for building design and code compliance. Data processing was limited to customary thermal design procedures in IP rather than SI units; more complex analytical techniques were not used. This evaluation technique should be familiar to most design professionals concerned with improving solar performance of light-frame wood construction. Information yielded by this study should not only be useful in developing new window-heat-recovery designs but also may lead to more reliable passive solar-performance predictions.

STUDY SITE AND STRUCTURES

The two test structures were at Farallones Institute Rural Center, located on the valley side of the California coastal mountain range west of Santa Rosa and east of Bodega Bay, approximately 10 miles from the Pacific coast at an elevation of 750 ft and latitude of 38.5° N. With a yearly degree-day total of about 3000, the local climate is relatively mild. The site does not experience much summer coastal fog, and the altitude places it just above the winter valley fog of the Santa Rosa area. The winter of 1977-78 (the test period), however, was unusually rainy, and performance of test structures was influenced by frequent cloudiness.

The study structures were built as living cabins for staff members and are typical of local design practices (Fig. 1, Tab. 1). The above-floor portion is built in light-frame wood construction with a plank-and-beam sleeping loft. The primary solar-heat storage system is of concrete slab floor construction. One cabin is representative of common passive solar design adaptations to wood-frame construction; heat is stored primarily by direct radiation received through windows, and it is identified as the "direct-gain cabin." The other structure represents an adaptation of the same architectural design to window heat recovery with no added heat storage mass and is identified as a "louver-window cabin."

Direct-Gain Cabin

The exterior walls of the direct-gain cabin are built with (all dimensions nominal) 4-in. [100 mm] wood studs, R-11 insulation, plywood sheathing, redwood board siding, and 1/2-in. [12 mm] gypsum wallboard interior finish. The flat lower roof is framed with 6-in. [150 mm] rafters and the upper barrel roof with 8-in. [200 mm] purlins. Both are insulated with R-19 glass fiber blankets, covered with plywood sheathing and roll roofing, and finished with redwood board ceilings. The sleeping loft is framed with redwood beams and a 2-in. [50 mm] pine deck left exposed. Windows are double glazed.

The floor system consists of a 3-in. [75 mm] concrete slab over 24 in. [600 mm] of pebble or river rock fill, 2- to 3- by 3/8-in. [50 x 75 x 9 mm] size. The storage bed is insulated with 2-in. [50 mm] polystyrene board on five sides and is surrounded by 8-in. [200 mm] concrete block foundation wall. The cabin was initially built for testing performance of the storage system with a convectively coupled flat-plate collector set on the natural slope at ground level; for the 1977-78 winter, however, the external collector was removed, and the cabin functioned fully in a direct-gain mode.

Louver-Window Cabin

Except for differences in window size and treatment, and a sloping rather than flat lower roof, the general construction details of the louver-window cabin are identical to those of the direct-gain cabin (Fig. 2).

The primary solar absorber surface is a narrow-slat venetian blind, dark green on one side and bright chrome on the other. The venetian blind serves not only as an absorber surface but also performs other window management functions. On cool days, it can be raised to maximize direct gain in the room, or it can be left partially open for control of direct-gain and remote- (or stored-) gain fractions. At night the closed blind can serve as a reflective surface for control of radiant heat losses across the window cavity.

The blind is installed in an airway between a double-glazed window and an interior glass panel. A 6-in.-wide [150 mm] opening along the top of the interior glass panel serves as the intake of room air for downward flow during the collection cycle and also permits removal of the blind. A circulating fan on the discharge side of the rock bed is thermostatically controlled by a sensor located at midheight of the louver-window airway. Heated air is collected

in a plenum at windowsill level and is then distributed across the storage bed through perforated 4-in. [100 mm] plastic drainpipe manifolds (Figs. 2 and 4). With downward airflow, storage becomes stratified vertically. Heat recovery from storage was purely passive by radiation and convection from the floor surface, and the rock-bed design minimized convective airflow to the room.

Building Thermal Properties

Heat flow and storage calculations are based on thermal properties determined in accordance with customary ASHRAE design procedures.[4] Because transitory effects present difficulties in determining building-envelope properties by field measurements, these estimates could not be validated experimentally.[5] The accuracy of calculated values, however, was considered adequate for the purposes of this study, which attempts to compare thermal performance of the two structures under essentially identical environmental conditions rather than to predict their energy requirements.

At the relatively protected test site, average wind speeds for the data-collection period were estimated at no more than 5 miles per hour and measured indoor-outdoor temperature differentials ranged around 20°F [11°C]. Because the cabins had no chimneys or other exhaust provisions, the average air-infiltration rate at test conditions was estimated at 0.2 air changes per hour (ach). If infiltration rates were assumed to vary proportionately with windspeeds and indoor-outdoor temperature differentials, the resulting air infiltration estimate would rise to 0.5 ach under more severe heating season average conditions in other localities.

Building heat-storage capacity and storage effects were based on isothermal mass assumptions (uniform temperature distribution) for any one mass element under consideration. Only those surfaces and materials directly exposed to daylight and to room air-temperature variations were presumed to be engaged in the heat-storage cycle. One notable exception, however, was the direct-gain cabin underfloor rock bed, where heat storage calculations were based on measured rock bed temperature variations, and the rock bed properties were considered in heat storage capacity calculations. As the louver-window cabin's rock bed is convectively coupled and stratified, its storage capacity was estimated in three layers, allowing consideration of stratification patterns.

RESEARCH METHODS

Experimental Procedures

The primary study objective was investigation of window heat-recovery performance rather than of solar performance of the cabins as such. Data collection, therefore, was largely limited to the heat storage system in floor construction, as this was recognized as the most critical component in studying the differences between the two structures. It should, however, be noted that the direct-gain cabin's floor-system thermocouples had been positioned in the given locations for previous studies.

Temperature measurements were used to study the response of the construction to changing thermal-load conditions. Temperatures of room air, floor surface, and rock bed were monitored with type "J" copper-constantan thermocouples; outdoor temperatures were measured with a shaded thermocouple. The direct-gain cabin was provided with nine data-collection points, and the louver-window cabin with 14 (Figs. 3 and 4, respectively). Hourly temperature measurements were recorded by a scanning multipoint recorder and later converted into temperature graphs by a computer-controlled plotter.

Solar radiation levels were monitored by a horizontally positioned outdoor pyranometer. Readings were integrated by electronic recorder to yield total daily radiation levels. For a more detailed performance evaluation, hourly radiation distribution patterns can be judged from variations in room-temperature profiles.

Analytical Procedures

In typical residential design, solar gains through windows are estimated on the basis of solar heat-gain factors[6] or similar procedures. Solar gains through opaque portions of the building envelope often are disregarded, or may be recognized in terms of reduced heat losses through application of "effective" heat loss coefficients. That method, however, is not suitable for more detailed thermal analysis of solar-heated structures and consideration of their dynamic performance patterns. Nevertheless, the simplicity of conventional steady-state design procedures does favor their use in analysis of buildings with lightweight envelopes.

Heat-storage effects in such construction can be recognized on the basis of procedures derived from conventional design methods.[7]

To allow application of steady-state design methods to this analysis, transitory response effects were damped by data averaging. Recorded hourly temperature variations were reduced to 8-hr averages representing a single solar heat collection cycle (08:00-16:00) and two recovery periods (16:00-24:00 and 24:00-08:00). Building and storage heat losses were estimated on the basis of average indoor-outdoor temperature differentials for any given cycle. Heat gain in, or recovery from, storage was estimated on the basis of storage temperature differentials between the end and the beginning of the cycle. Storage calculations were based on lumped and isothermal mass assumptions. For the wood-frame construction portion (above-floor line), where direct temperature measurements were not available, mass temperature variations were equated with room air temperature variations.

Room and storage temperature measurements allowed calculation of the energy expended in maintaining the observed indoor-outdoor temperature differentials and increasing the heat content of storage. After appropriate reductions for other heat input, that quantity of energy was identified as the "useful solar gain." Where such gain led to an excessive room temperature rise, it was no longer considered truly "useful," and adjustments were made to approximate quantities of useful solar gain at controlled room temperature. More detailed discussion of this analytical method follows. For clarity, the discussion is organized in a somewhat different sequence from the actual analytical procedure.

Solar performance evaluation. A major objective in solar collector design is control of collection losses attributable to reflections from the absorber surface and to overheating of the glass cover. Solar-collector efficiency is expressed as a ratio of collected to incident energy. The same concept has also been adapted to solar-oriented buildings, and typical design procedures rely on use of space absorption coefficients for estimating solar heat gains from calculations of solar radiation received through glass. The analytical method used in this study, on the other hand, allows calculation of a "solar gain ratio" as an experimental solar performance measure that corresponds to the somewhat arbitrarily chosen space absorption coefficients. The solar gain ratio (SGR) is a dimensionless quotient of useful (Q_{SU}) and nominal (Q_{SN}) solar gains, measured in Btu [kW·hr]/day:

$$SGR = Q_{SU}/Q_{SN} \tag{1}$$

The nominal solar gain estimate corresponds to customary calculations of energy received through glass before application of absorption coefficients. Actual collection losses (or the numerical difference between Q_{SU} and Q_{SN}) commonly remain unquantified.

Useful solar gain. Estimates of useful solar gains were based on the calculations of the corresponding heat losses (Q_{HL}, in Btu [kW·h]), the net heat gain in or loss from storage (Q_{HS} in Btu [kW·hr]) for the study period, and other heat gains (Q_{HG}, in Btu [kW·hr]):

$$Q_{SU} = Q_{HL} + Q_{HS} - Q_{HG} \tag{2}$$

With no net change in storage heat content ($Q_{HS} = 0$) and no other gains ($Q_{HG} = 0$), the expression is reduced to

$$Q_{SU} = Q_{HL} \tag{3}$$

Nominal solar gain. The method for calculating nominal solar gains is derived from customary solar design practices. Integrated measurements of solar radiation received in a horizontal plane (H, in Btu/ft²·day [W/m²·day]) were converted into vertical radiation components that also include ground reflectance effects. The vertical-to-horizontal radiation ratios (R, dimensionless) for different orientations were extrapolated from average day radiation data by Kusuda and Ishii[8] for localities of comparable latitude and sky conditions. The estimated ratios for January are 1.40 for south glass, 0.64 for east and west glass, and 0.32 for north glass. For recognition of diffuse radiation effects, average rather than clear-day references were used.

For orientations other than south, only glazed openings were considered in calculation of solar gains. Estimates for south glass, on the other hand, also include gains through south-facing roof and wall surfaces expressed in terms of "equivalent glass area." The conversion procedure is derived from the ASHRAE method for cooling load calculations.[9] The resulting solar aperture is identified as "design glass area" (DGA, in ft² [m²]). The conversion

allows calculating gains through opaque surfaces on the basis of the same radiation data as applied to glazed openings, rather than on conventionalized sol-air temperatures. In such calculations, the assumed average glass transmittance $\bar{\tau}$ of 0.78 (as for double glazing) applies to both actual and "equivalent" glass areas.

With introduction of a time factor (T, in days), the calculation is

$$Q_{SN} = H \times R \times DGA \times \bar{\tau} \times T \tag{4}$$

The nominal solar gain calculated without further absorption coefficients implies that radiation is "received through glass" rather than "received by the space as a collector."

Recovery-cycle heat balance. During the recovery periods (16:00-24:00 and 24:00-08:00), there is no solar gain ($Q_{SU} = 0$). In case of no other heat gains ($Q_{HG} = 0$), heat losses must be limited to the level of heat recovered from storage

$$Q_{HL} = Q_{HS} \tag{5}$$

This relationship allows mutual validation of both calculations because they are based on different sets of data. The heat loss estimate is a product of the building heat loss rate (q_{hl}, in Btu/hr·°F [W·°C]), the average indoor-outdoor temperature differential ($\bar{t}_i - \bar{t}_o$, in °F [°C]) for the period of investigation, and the length of that period (in hours). Calculations of stored heat recovery, on the other hand, are based on storage capacity (C_{hs}, in Btu/°F [kW·hr/°C]) and the differential between beginning (t_{sb}) and ending (t_{se}) storage temperatures (in °F [°C]) for the given period. Disagreements between heat loss and storage calculations for any recovery period are identified as "closure errors" (CE). With such substitutions, Eq. 5 becomes

$$q_{hl}(\bar{t}_i - \bar{t}_o)\, h = C_{hs}(t_{sb} - t_{se}) + CE \tag{6}$$

It must be noted that, for the above-floor (wood construction) portion, losses from storage are included with building heat losses. Those losses for the below-floor (floor slab and rock bed) portion were estimated separately and subtracted from the total change in storage heat content in calculating of heat recovered to the room. The collection cycle total heat gain in storage was estimated on the basis of the corresponding daytime temperature change ($t_{se} - t_{sb}$), and the corresponding storage losses to outdoors were added to the net heat gain in storage for calculations of useful solar gain.

Adjustments to useful solar-gain estimates. Direct-gain solar designs often suffer from excessive daytime room temperature swings, in which the human comfort range and the limits defined by energy performance standards are exceeded. While sun and temperature control can be achieved by shading and ventilation, the resulting reduction in daytime temperature also leads to a corresponding loss of heat that could have been stored for later recovery. In this study, the direct-gain cabin temperatures exceeded an allowable range and, for performance comparisons, were reduced to the more acceptable louver-window cabin temperature range. Reduced or adjusted data are identified by a superscript ('). The procedure for estimating adjusted useful solar gains (Q'_{SU}) is derived from Eq. 2. The high room temperature is equated with indoor temperature at the end of the collection cycle (t_{ie}) and low room temperature with that at the beginning of the collection cycle (t_{ib}). For the purposes of this study, the reduction in heat stored for later recovery was equated with differences between measured and adjusted collection-cycle room temperatures. In a simplified form, where Q_{HLc} represents collection cycle heat losses and Q_{HS} represents recovery-cycle heat losses (thus assuming no change in storage heat content for that day or period of investigation), the adjusted useful solar gain calculation can be derived from Eq. 2 as:

$$Q'_{SU} = Q_{HLc}\left(\frac{\bar{t}'_i - \bar{t}_o}{\bar{t}_i - \bar{t}_o}\right) + QHS\left(\frac{t'_{ie} - t'_{ib}}{t_{ie} - t_{ib}}\right)' - Q_{HG} \tag{7}$$

Mechanical efficiency estimates. The coefficient of performance (COP) of the fan-assisted louver-window heat-collection system was calculated as a ratio of the difference in collected energy between unadjusted and adjusted useful solar gain estimates to mechanical energy expended (Q_{ME}, in Btu [kW·hr]) to gain the measured improvement:

$$COP = \frac{Q_{SU} - Q'_{SU}}{Q_{ME}} \qquad (8)$$

RESULTS

Variations in outdoor temperature and solar-radiation levels or distribution can lead to a variety of transitory response effects that are difficult to recognize and eliminate. To minimize the impact of such variables, analysis was extended from the customary "design day" to a 5-day period. The given period, furthermore, was chosen for its relatively consistent outdoor temperature profiles and solar radiation levels.

Experimental Data

Direct-gain cabin temperature profiles are shown in Figs. 5 and 6, and those of the louver-window cabin are in Figs. 7 through 9. Outdoor temperature profiles and daily solar radiation measurements are shown in Figs. 5 and 7. For performance analysis under "adjusted" temperature conditions the indoor temperature profiles for the two cabins (Figs. 5 and 7) were interchanged, as if to be applicable to the direct-gain cabin with shading and to the louver-window cabin in direct-gain mode (venetian blind raised).

Direct-gain cabin air temperatures (Fig. 5) show a relatively steady indoor-outdoor temperature differential during the recovery cycle but rapid indoor temperature rise during the collection cycle. Rock bed temperature variations (Fig. 6) agree in cycle with floor slab temperature variations (Fig. 5) but show remarkable variations at point 20, which falls below a section of floor slab exposed to direct sunlight for more than a 4-hr period. Shadow lines cast by the window frame between 10:00 and 14:00 are shown in Fig. 3. The significance of these observations is discussed under direct-gain cabin "Underfloor Storage Performance."

Louver-window cabin air temperature profiles (Fig. 7) show a more moderate rise during the collection cycle and a relatively steady indoor-air floor-slab temperature differential during the recovery cycle. Louver-window temperature profiles are shown in Fig. 8. The heat-recovery system is controlled by a thermocouple at midheight of the window cavity, activating a circulating fan at temperatures above 90° F [32°C]. Effects of fan operation are evident from crossover of window top and bottom temperature profiles. With downward airflow, the top of the window cavity is cooled by entering room air, but the temperature at the bottom continues to rise with increasing solar intensity level. Point 57 shows the approximate temperature of air entering the rock bed. During the night, the cavity becomes stratified and the average temperature at midheight falls close to indoor air temperature, suggesting that nighttime heat losses through the window can be estimated on the basis of a simple indoor-outdoor temperature differential.

The louver-window cabin's rock-bed temperatures are shown in Fig. 9. Points 44 and 49 (Figs. 4 and 9) lie directly above the air manifold and show good agreement with slab-temperature variations at the corresponding points 55 and 54 (Fig. 7). Point 39 is between the manifold pipes and gains heat more slowly. During heat recovery, on the other hand, stagnant air in the manifold acts as an insulator, and upward heat flow at points 44 and 49 is retarded. Similar variations in temperature profiles at other depths (Fig. 9) show the influence of variations in rock bed density and apparent formation of a cooler air zone above point 40 during the night, but such variations appeared to have no further significance in the overall performance of the system.

Analytical Data

Recorded temperature measurements were reduced by averaging to single-point references for any one zone, such as the direct-gain cabin's indoor air or middle of the louver-window cabin's rock bed. Data were then processed in accordance with Eqs. 1 through 8. Results of thermal-performance calculations for both cabins are summarized in Tab. 2, and heat balance calculation summaries for each 8-hr period are shown in Tabs. 3 and 4.

Other Heat Sources

Other heat inputs were not monitored and, therefore, are recognized only by averaged values; daily departures from such averages may be reflected in the closure error. The direct-gain cabin served as sleeping quarters for one person, and the body heat output was estimated at 275 Btu/hr [81 W], or 4400 Btu [1.29 kW·hr] for the 16-hr recovery period. Its low temperatures were also boosted by a portable electric heater, having an average output estimated at 2200 Btu [0.65 kW·hr] per night. The louver-window cabin required electricity for its 1/6-hp air-circulating fan, estimated at 2000 Btu [0.6 kW·hr] for the average 5-hr period of fan operation. As the fan heat became part of the collection-cycle heat input, it was subtracted from the total heat gain in calculation of useful solar heat gains.

Magnitude of Closure Error

The residual termed "closure error" is indicative of transient response effects that remained undetected by the experimental and analytical methods used. The magnitude of such daily residuals, expressed as a percentage of the estimated recovery cycle heat loss, for the direct-gain cabin ranged from -4.4% to +9.8% and the for 5-day average was -3.5%. Corresponding values for the louver-window cabin ranged from -19% to +17% with an average of 0.8%. The relatively insignificant 5-day average values suggest satisfactory damping of transients over that period.

DISCUSSION

Agreement With Conventional Design Methods

For a test of validity, solar-gain ratios estimated by the method used in this study were compared against values of absorption coefficients commonly used in passive solar design. Such coefficients range from 0.95 for a flat black collector plate to 0.85 to 0.75 for interior room surfaces. The value of 0.95 is also gaining popularity in direct-gain passive solar design as an overall space absorption coefficient, although this value may be too high for less-than-ideal conditions (including dust on glass). With Q_{SN} calculations also including gains through opaque surfaces (about 6% of total for the direct-gain and 3% for the louver-window cabin), SGR values could be expected to fall in the range of 0.9 to 0.8. The calculated 5-day average SGR for the direct-gain cabin is 0.89 and for the louver-window cabin 0.84. Thus, agreement with expected values based on analogy with conventional design coefficients is satisfactory.

Direct Gain Cabin Performance

Room temperature fluctuations. The recorded low and high room temperatures for the 5-day period were 58°F [14.4°C] and 87°F [30.6°C], respectively. The 5-day average low and high temperatures were 59.2°F [15.1°C] and 82.1°F [27.8°C], with an average room temperature swing of 22.9°F [12.7°C]. The 5-day average room temperature was 69.1°F [20.6°C], and, at an average outdoor temperature of 47.8°F [8.8°C], the temperature differential sustained with solar and auxiliary heat was 21.3°F [11.8°C].

Underfloor storage performance. Rock-bed temperature fluctuations at point 20 (Figs. 3 and 6), below a sunlit portion of floor slab, suggest that such construction can serve as a responsive solar heat storage medium. Temperature rise at other rock-bed points (21 and 22) is far lower and shows that storage capacity remaining outside the range of direct solar radiation is poorly utilized. The relatively rapid downward flow of heat at point 20, however, also suggests that the slab was overheating and just as rapidly losing heat to room air above. Measurements of slab temperature for verification of this assumption were not available, but, by comparison with slab temperature variations at points 23 and 24 (Figs. 3 and 5), it can be concluded that excessively prolonged exposure to direct sunlight may be no more advantageous than the lack of such exposure. From a practical house-design standpoint, positioning windows for effective distribution of sunlight may be a difficult task, and the direct-gain passive solar design concept with concrete floor slab for heat storage does not seem as advantageous as the alternate choice of window heat recovery.

Solar design efficiency. The daytime room temperature fluctuations averaging 22.9°F [12.7°C] exceeded the 15°F [8.3°C] range commonly considered an acceptable target in passive solar design. The 82.1°F [27.8°C] average high temperature also exceeded that allowed by some regulatory standards.[10] The sensation of comfort at 82°F [27.8°C] with normal indoor clothing,

expressed in terms of Predicted Mean Vote,[11] however, would fall in the range of only "slightly warm," rather than "hot." Nevertheless, for impartial performance evaluation, room temperature excursions must be reduced to a range recognized by standards.

For this study, the most useful basis for comparison is the louver-window cabin temperature range, which did fall within recognized limits. The measured louver-window cabin temperatures, therefore, can be applied as "adjusted" temperatures in the analysis of the direct-gain cabin. Equation 7 then yields a 5-day average of Q'_{SU} = 40,120 Btu [11.8 kW·hr], and Eq. 1 a 5-day average of SGR' = 0.59. Although the average 24-hr heat loss has also been reduced to Q'_{HL} = 60,870 Btu [17.8 kW·hr], the solar contribution now meets only 66% of that load, compared to 88% under the full measured temperature excursions.

Comparison of the direct-gain cabin's performance data at different operating temperatures shows the importance of good design for temperature control. Although operating temperatures could also have been reduced by added mass rather than by shading, temperature profiles for mass out of direct sunlight (Fig. 5, point 23) show the importance of strategic placement for thermal mass to yield its full benefits in direct-gain design.

Louver-Window Cabin Performance

Room temperature fluctuations. Indoor temperature profiles show relatively constant swings averaging 12.7°F [7.1°C] over the 5-day period. The average 08:00 temperature, sustained with only solar heat, was 60°F [15.6°C]; room temperature fell somewhat below that level on only one day. The recorded high room temperature was 75.5°F [24.2°C], with a 5-day average high at 72.7°F [22.6°C]. The average indoor temperature was 66.5°F [19.2°C], for an 18.7°F [10.4°C] average indoor-outdoor temperature differential.

Under-floor storage performance. The vertically stratified rock bed showed variations in internal temperature distribution but produced acceptably uniform floor-slab temperatures (Fig. 7, points 54 and 55). Heat recovery from storage required no supplementary energy (as compared to the storage cycle). The floor slab performed as a radiant panel maintaining a relatively steady 10°F [5.6°C] temperature differential between floor surface and room air for the entire recovery cycle. Estimates of average heat-recovery rate from the floor slab to room air show close agreement with theoretical slab heat-release rate calculations based on ASHRAE design procedures.[12] Actual heat recovery from under-floor storage to room was estimated as the difference between a change in storage heat content and direct heat loss from storage to outdoors for the 16:00-08:00-hour recovery period. The resulting 5-day average heat-recovery rate is 49,710 Btu/day [14.6 kW·hr/day] or 3,110 Btu/hr [911 W]. The theoretical heat-recovery-potential estimate is based on slab surface properties. The surface area exposed to room air can be approximated at 178 ft² [16.6 m²], corresponding to 196 ft² [18.2 m²] nominal floor area reduced by the perimeter band of nominal 4-in. [100 mm] wall construction. At an emission rate of 1.63 Btu/hr·ft²·°F [9.24 W/m²·°C] and a 10°F [5.6°C] slab-to-air temperature differential, the theoretical heat release rate would be 2900 Btu/hr [850 W].

Collection cycle (08:00-16:00) performance reveals probable weaknesses in the given rock-bed design. While the louver-window cabin daytime temperatures rise less rapidly than those of the direct-gain cabin, the recorded rate of temperature rise of more than 3°F [1.7°C] per hour still is somewhat steeper than desirable for comfort and effective solar-gain management. Although the circulating fan helps to cool the room with air from the lower level of the rock bed, averaging 67°F [19.5°C], rapidly rising slab temperatures also suggest immediate heat gain from the slab to room air. It is possible that the upward heat flow could have been retarded by setting the top manifold somewhat lower in the rock bed.

As temperature variations in the lower two-thirds of the rock bed were less pronounced than those near the top, much of the available mass did not store recoverable heat in the floor-slab temperature range. The cool mass, however, helped to control room temperatures during the collection cycle by extracting the residual window heat from the circulating airflow.

Solar design efficiency. As room temperatures for the 5-day period fell within an acceptable range, the calculated SGR of 0.84 can be considered valid. A better performance indicator, however, is the efficiency rating of its fan-assisted solar collection fraction. Performance of a window heat recovery system could be evaluated by comparative heat-balance calculations on similar days with the fan operating and not operating. Variability in weather during the winter of 1977-78, however, did not allow such studies. As an alternative, predicted solar performance of the louver-window cabin in a direct-gain mode (with the venetian blind partly or fully raised) was extrapolated by analogy with the direct-gain cabin.

It can be assumed that at some venetian blind settings, louver-window cabin's daytime temperature variations would be comparable to those of the direct-gain cabin under similarly controlled "adjusted" temperatures. At that level, their adjusted SGR' values and reduction in heat stored for later recovery should also be comparable. Similarly, both cabins would require comparable auxiliary heat input for maintaining night temperatures at the desired level. On the basis of such analogy, the adjusted useful solar gain for both cabins can be estimated at Q'_{SU} = 40,120 Btu [11.8 kW·hr] as computed previously for the direct-gain cabin. The original 5-day average useful solar gain value for the louver-window cabin is Q_{SU} = 86,810 Btu [25.4 kW·hr]. The improvement attributable to fan assistance, therefore, may be expressed by the difference between these two values. The coefficient of performance for the fan-assisted system requiring a 2000-Btu [0.6 kW·hr] input can be estimated in accordance with Eq. 8 as

$$COP = \frac{86,810 - 40,120}{2000} = 23.3$$

One of the key factors contributing to the overall effectiveness of the system was the performance of the venetian blind as an absorber surface. It led to approximately a 40°F [22°C] air temperature rise on a single pass (Fig. 7, 68°F [20°C] room air to 108°F [42°C] bottom of louver-window temperature at 13:00 on January 25). It also appeared to serve as an efficient divider of solar gain between storage and room air. It is entirely possible that the venetian blind used as an energy management tool could have led to still higher useful solar gain levels. Such management strategies could reduce reflections from the blind back through glass and increase the direct gain fraction at appropriate times. These possibilities, however, were not investigated.

Economic considerations. The louver-window cabin was built by Farallones Institute students as part of a larger appropriate technology demonstration project. Full cost data are not available, but the direct cost, including materials, equipment rental, and subcontracts, was $8980. The cost of major items attributable to the window heat-recovery system (blower with controls, air manifold pipe, 3/16-in. [5 mm] interior glass panels, and venetian blinds) was less than $300, or 3.3% of the direct cost. If the venetian blind is viewed as part of basic construction needed for window control and privacy, the cost of the special window-heat-recovery items is reduced to 2% of the louver-window cabin's direct cost.

CONCLUSIONS

The study yielded new information on the performance of light-frame wood structures in a solar design environment and on the potential for improving their performance through window heat recovery. Although the two study structures were comparable in their inherent thermal properties, and differed only in solar rather than in architectural design concepts, the window heat recovery (louver-window) structure performed markedly better than the direct-gain structure. More detailed conclusions from this study include:

1. The direct-gain cabin's rock bed was engaged in the daily heat storage cycle, but mass in direct sun performed more efficiently than that out of the sun. The resulting overheating was attributable to a poor coupling between load and storage mass rather than to insufficient heat-storage capacity. Adjustments for overheating led to a marked reduction in the fraction of heating load estimated to be met by solar gains.

2. The louver-window cabin's rock bed was engaged in the daily cycle by forced airflow, effectively increasing the available heat-storage capacity. Resulting room temperature swings were less objectionable, and the estimated solar heating fraction was correspondingly higher. The coefficient of performance for the fan-assisted window heat-recovery system was deemed high enough to justify such expenditure of electrical energy.

3. Modifications needed for window heat recovery were easily integrated into the existing architectural design of the study structures. The louver-window cabin's thermal performance was improved without increasing its inherent thermal mass or departing from basic light-frame wood construction practices. Observations suggest that window heat recovery can help to overcome restrictions that may be imposed by regulatory standards on use of solar design details in light-frame wood construction.

NOMENCLATURE

H	daily solar radiation received on horizontal plane, Btu/ft^2·day [W/m^2·day]
R	vertical-to-horizontal radiation ratio for the conditions, dimensionless
T	time factor, day
hr	time factor, hr
$\bar{\tau}$	average glass transmittance factor, dimensionless
C_{hs}	heat storage capacity, Btu/°F [kW·hr/°C]
Q_{HG}	internal heat gain, Btu [kW·hr]
Q_{HL}	heat loss from building and storage to outdoors, Btu [kW·hr]
Q_{HLc}	collection cycle heat loss to outdoors, Btu [kW·hr]
Q_{HS}	heat gain in or loss from storage, Btu [kW·hr]
Q_{ME}	mechanical energy expended, Btu [kW·hr]
Q_{SN}	nominal solar heat gain, Btu [kW·hr]
Q_{SU}	useful solar heat gain, Btu [kW·hr]
q_{hl}	heat loss rate, Btu/hr·°F [W·°C]
t_i	average indoor temperature, °F [°C]
$\bar{t}_o$	average outdoor temperature, °F [°C]
t_{ib}	beginning indoor air temperature, °F [°C]
t_{ie}	ending indoor air temperature, °F [°C]
t_{sb}	beginning isothermal storage temperature, °F [°C]
t_{se}	ending isothermal storage temperature, °F [°C]
CE	closure error, dimensionless
COP	coefficient of performance, dimensionless
DGA	design glass area, ft^2 [m^2]
SGR	solar gain ratio, dimensionless
superscript (')	analytically adjusted values

REFERENCES

1. U.S. Department of Agriculture, Farmers Home Administration, "Conservation of Petroleum and Natural Gas Through Proposed Changes in USDA Financial Assistance Programs," Federal Register 90:(45) (May 1980) p. 30364-30366.

2. E. Mazria, The Passive Solar Energy Book (Emmaus, PA: Rodale Press, 1979.

3. D. Watson, Designing and Building a Solar House (Charlotte, VT: Garden Way Publishing, 1977).

4. ASHRAE Handbook--1981 Fundamentals (Atlanta, GA: ASHRAE, 1981).

5. P. Calthorpe, B. Wilcox, and D. Staufer, The Farallones Institute Solar Study (Occidental, CA: The Farallones Institute, 1978).

6. ASHRAE Handbook--1981 Fundamentals (Atlanta, GA: ASHRAE, 1981).

7. G. Hans, "Proposed Streamlined Residential Heating Energy Budget Analysis by a Variable Temperature Design Method," ASHRAE SP 28, Proceedings of the ASHRAE/DOE-ORNL Conference (Atlanta, Ga: ASHRAE, 1979).

8. T. Kusuda, and K. Ishii, "Hourly Solar Radiation Data for Vertical and Horizontal Surfaces on Average Days in the United States and Canada," Building Science Series No. 96 (Washington, DC: U.S. Dept. of Commerce, National Bureau of Standards, 1977).

9. Hans, 1979.

10. U.S. Department of Agriculture, 1980.

11. ASHRAE Handbook--1981 Fundamentals, Chapter 8, p. 8.25.

12. ASHRAE Handbook--1981 Fundamentals, Chapter 23, p. 23.9,12.

13. P. Calthorpe, Farallones Institute Solar Data Package and Performance Analysis: Final Report (Berkeley, CA: Peter Calthorpe, 1980).

TABLE 1
Study Structure Properties[1]

Parameter	Direct-Gain Cabin	Louver-Window Cabin
Solar design concept	Direct gain passive	Window heat recovery
Solar heat absorber	Interior and south-facing exterior surfaces	Venetian blind; also interior and south-facing exterior surfaces
Solar heat storage	Inherent thermal mass, including floor system	Underfloor rock bed and inherent building thermal mass
Solar heat collection mechanism	Direct radiation and natural convection	Thermostatically controlled airflow and direct radiation
Solar heat recovery mechanism	Natural radiation and convection	Natural radiation and convection
Temperature control system	None on collection, boost by heater on recovery	Indirect (window temperature) on collection, none on recovery
Main floor area	196 ft^2	196 ft^2
Total window area	87 ft^2	129 ft^2
South glass area	60 ft^2	102 ft^2
South design glass area, DGA	64.5 ft^2	105.2 ft^2
Heat loss rate	131 Btu/hr·°F	154 Btu/hr·°F (recovery period)[2]
Heat storage capacity	6060 Btu/°F	8300 Btu/°F[3]

[1]Applicable IP/SI conversion factors:

$ft^2 = 0.0929\ m^2$

Btu/hr·°F = 0.527 W/°C

Btu/°F = 0.527 W·hr/°C

Btu/lb·°F = 1.16 W·hr/kg·°C

[2]Louver-window cabin heat losses for the recovery period are calculated on the basis of average indoor air temperatures for both louver window and other parts of the building envelope; for the collection period, louver-window losses are estimated on the basis of 90°F (32°C) average temperature and for other parts of the envelope on the basis of average indoor air temperature.

[3]Heat-storage capacity of wood estimated at 0.375 Btu/lb·°F for 10% moisture content. Rock-bed heat-storage capacity estimated at full 24-in. [600 mm] depth for the louver-window cabin and at reduced 18-in. [450 mm] depth for the direct-gain cabin. Above-floor heat-storage capacity estimate applies to only those materials directly exposed to room air, and includes a further 15% allowance for furniture.

TABLE 2
Thermal Performance Summary[1]

Parameter	Direct-Gain Cabin	Louver-Window Cabin
Average heat loss, Q_{HL}	-67,030 Btu/day	-84,310 Btu/day
Fan energy provided	0	2000 Btu/day
Other heat input	6600 Btu/day	0
Average net storage gain, Q_{HS}	1730 Btu/day	4100 Btu/day
Average closure error, CE	1640 Btu/day	-400 Btu/day
Average useful gain, Q_{SU}	60,510 Btu/day	86,810 Btu/day
Average nominal gain, Q_{SN}	67,910 Btu/day	103,300 Btu/day
Average gain ratio, SGR	0.89	0.84
Recorded high temperature	87°F [30.6°C]	75.5°F [24.2°C]
Recorded low temperature	58°F [14.4°C]	59°F [15.0°C]
Average high room temperature	82.1°F [17.8°C]	72.7°F [22.6°C]
Average low room temperature	59.2°F [15.1°C]	60.0°F [15.6°C]
Average room temperature swing	22.9°F [12.7°C]	12.7°F (7.1°C]
Adjusted Q'_{SU}[2]	40,120 Btu/day	
Adjusted SGR'[2]	0.59	
Solar contribution, Q_{SU}		
Test conditions	88% of Q_{HL}	98% of Q_{HL}
Adjusted conditions	66% of Q_{HL}	

[1]Applicable IP/SI conversion factors:
Btu/day = 2.93×10^{-4} kW·hr/day
°C = (°F-32) 5/9
[2]Estimated for temperatures measured in the louver-window cabin.

TABLE 3
Direct-Gain Cabin Daily Performance[1]

Date	Cycle	Q_{HL}	Q_{HS}[2]	Q_{HG}	CE[3]	Q_{SU}[4]	Q_{SN}	SGR
				Btu				
January								
25-26	08:00-16:00	22,530	+29,060	--	--	51,590	72,500	0.71
	16:00-24:00	23,580	-17,210	2,200	+4,170	--	--	--
	24:00-08:00	18,860	-17,430	4,400	-2,960	--	--	--
	Daily total	64,970	-5,580	6,600	+1,210	--	--	--
26-27	08:00-16:00	20,960	+45,950	--	--	66,910	69,630	.96
	16:00-24:00	26,200	-21,910	2,200	+2,090	--	--	--
	24:00-08:00	20,440	-19,510	4,400	-3,470	--	--	--
	Daily total	67,600	+4,530	6,600	-1,380	--	--	--
27-28	08:00-16:00	19,180	+34,670	--	--	53,850	64,390	.84
	16:00-24:00	24,000	-17,770	2,200	+4,030	--	--	--
	24:00-08:00	17,920	-12,840	4,400	680	--	--	--
	Daily total	61,100	+4,060	6,600	+4,710	--	--	--
28-29	08:00-16:00	19,910	+41,870	--	--	61,780	63,890	.97
	16:00-24:00	24,630	-21,410	2,200	+1,020	--	--	--
	24:00-08:00	18,860	-17,400	4,400	-2,940	--	--	--
	Daily total	63,400	+3,060	6,600	-1,920	--	--	--
29-30	08:00-16:00	20,960	+47,480	--	--	68,450	69,140	.99
	16:00-24:00	29,340	-23,940	2,200	+3,200	--	--	--
	24:00-08:00	27,770	-20,980	4,400	+2,390	--	--	--
	Daily total	78,080	+2,560	6,600	+5,590	--	--	--
25-30		--	+8,630	--	--	--	--	--
	Average	67,030	+1,730	6,600	+1,640	60,510	67,910	.89

[1] Q_{HL} = heat loss for cycle and total heat loss for the day; Q_{HS} = change in storage heat content for cycle and net change for day; Q_{HG} = heat gained from internal and auxiliary heat sources; CE = closure error (difference between heat loss and input); Q_{SU} = useful solar gain; Q_{SN}: nominal solar gain; SGR = useful-to-nominal solar gain ratio.

Applicable IP/SI conversion factor: Btu = 2.93 x 10^{-4} kW·hr

[2] + denotes heat gain in storage; - denotes recovery from storage; 5-d gain indicates net increase in heat content.

[3] + indicates greater calculated heat loss than recovery; - indicates greater recovery than heat loss.

[4] Q_{SU} value on line 08:00-16:00 calculated from daily totals as:

$$Q_{SU} = Q_{HL} + Q_{HS} - Q_{HG} - CE$$

TABLE 4
Louver-Window Cabin Daily Performance[1]

Date	Cycle	Q_{HL}	Q_{HS}[2]	Q_{HG}	CE[3]	Q_{SU}[4]	Q_{SN}	SGR
		- - - - - - - - - - - - - Btu - - - - - - - - - - - - -						
January								
25-26	08:00-16:00	32,260	+52,030	2,000	--	82,290	110,280	0.75
	16:00-24:00	28,020	-28,280	--	-260	--	--	--
	24:00-08:00	26,640	-24,840	--	+1,800	--	--	--
	Daily total	86,920	-1,090	2,000	+1,540	--	--	--
26-27	08:00-16:00	32,600	+66,750	2,000	--	97,350	105,920	.92
	16:00-24:00	28,570	-35,980	--	-7,410	--	--	--
	24:00-08:00	27,300	-30,710	--	-3,410	--	--	--
	Daily total	88,470	+60	2,000	-10,820	--	--	--
27-28	08:00-16:00	33,350	+48,540	2,000	--	79,890	97,950	.82
	16:00-24:00	26,010	-27,820	--	-1,810	--	--	--
	24:00-08:00	23,270	-26,320	--	-3,050	--	--	--
	Daily total	82,630	-5,600	2,000	-4,860	--	--	--
28-29	08:00-16:00	29,600	+60,970	2,000	--	88,570	97,200	.91
	16:00-24:00	24,100	-23,430	--	+670	--	--	--
	24:00-08:00	23,730	-21,840	--	+1,890	--	--	--
	Daily total	77,430	+15,700	2,000	+2,560	--	--	--
29-30	08:00-16:00	30,500	+57,430	2,000	--	85,930	105,170	.82
	16:00-24:00	28,630	-23,370	--	+5,260	--	--	--
	24:00-08:00	26,960	-22,620	--	+4,340	--	--	--
	Daily total	86,090	+11,440	2,000	+9,600	--	--	--
25-30		--	+20,510	--	--	--	--	--
	Average	84,310	+4,100	2,000	-400	86,810	103,300	.84

[1] Q_{HL} = heat loss for cycle and total heat loss for the day; Q_{HS} = change in storage heat content for cycle and net change for day; Q_{HG} = heat gained from internal and auxiliary heat sources; CE = closure error (difference between heat loss and input); Q_{SU} = useful solar gain; Q_{SN} = nominal solar gain; SGR = useful-to-nominal solar gain ratio.

Applicable IP/SI conversion factor: Btu = 2.93 x 10^{-4} kW·hr

[2] + denotes heat gain in storage; - indicates recovery from storage; 5-day gain indicates net increase in heat content.

[3] + indicates greater calculated heat loss than recovery; - indicates greater recovery than heat loss.

[4] Q_{SU} value on line 08:00-16:00 calculated from daily totals as

$$Q_{SU} = Q_{HL} + Q_{HS} - Q_{HG} - CE$$

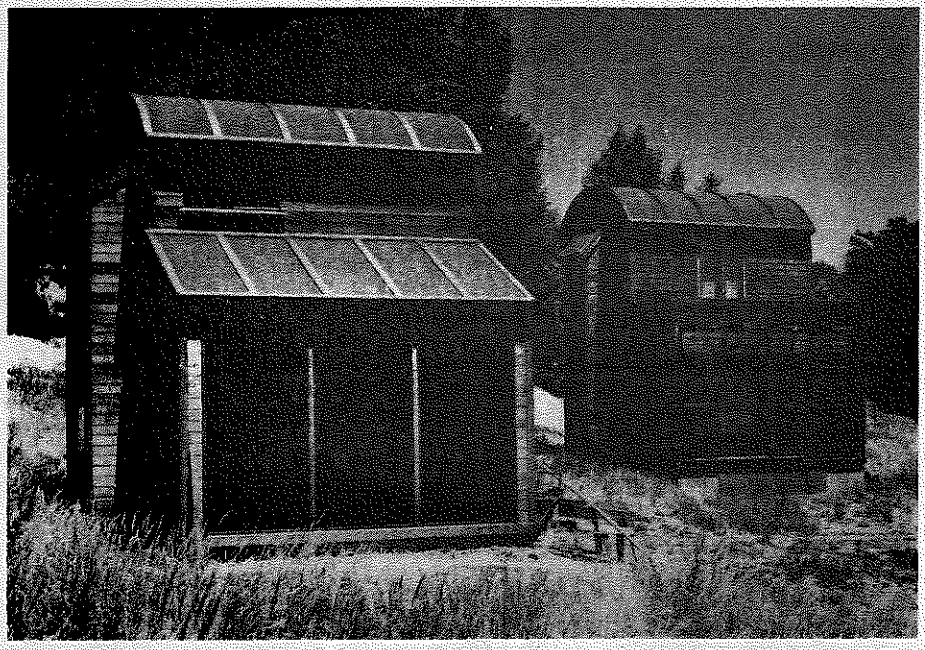

Figure 1. South-southwest view of study structures (louver-window cabin, left; direct-gain cabin, right)

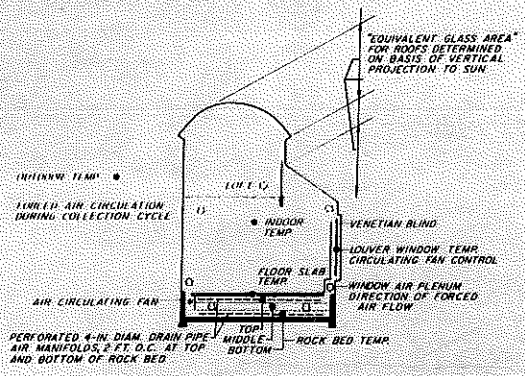

Figure 2. Diagrammatic cross section of louver-window cabin. (Direct-gain cabin is similar except for the absence of the forced-flow window heat recovery system)

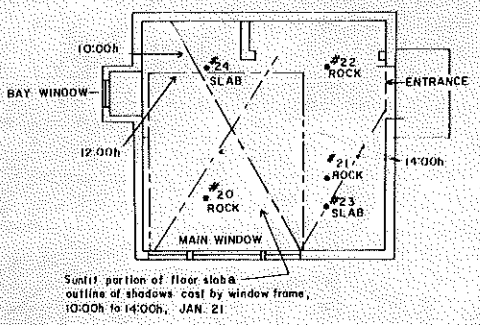

Figure 3. Floor plan and data points of the direct-gain cabin. Data point 20 at middepth of the rock bed falls below floor slab that on Jan. 21 is exposed to direct sunlight for more than a 4-hour period. There also is a high window to the right of the main window (see Fig. 1) so that floor slab at the rear of cabin is also exposed to direct sunlight for part of the time

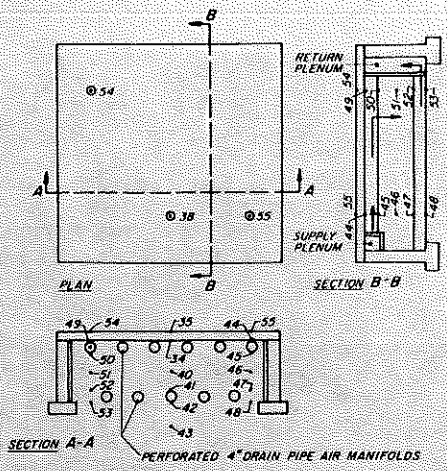

Figure 4. Rock-bed layout and data points of the louver-window cabin

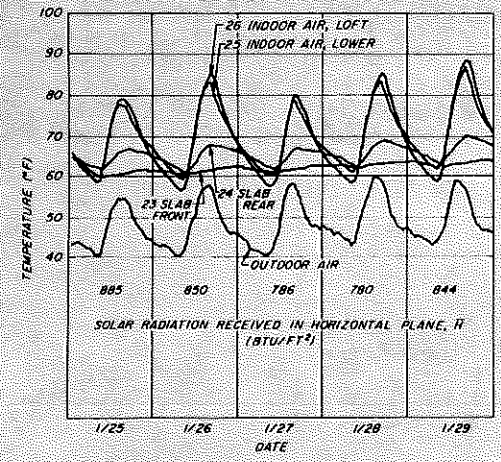

Figure 5. Indoor temperature profiles and outdoor conditions of the direct-gain cabin

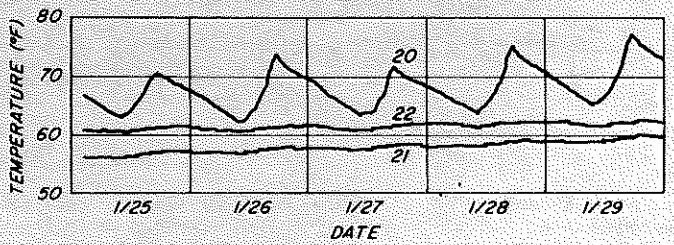

Figure 6. Rock-bed temperatures (location of points shown in Fig. 3) of the direct-gain cabin. Profiles show rock-bed temperature variations at middepth of rock bed (12 in. below floor slab). Point 20 falls below floor slab exposed to direct sunlight for more than a 4-hour period. Slab above point 22 is exposed to sun only after 12:30, and that over point 21 after 13:30

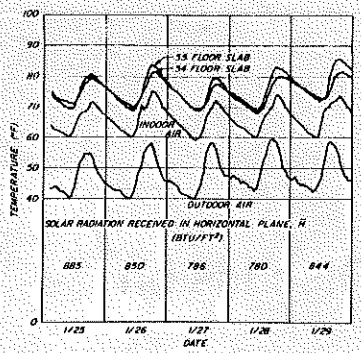

Figure 7. Indoor temperature profiles and outdoor conditions of the louver-window cabin

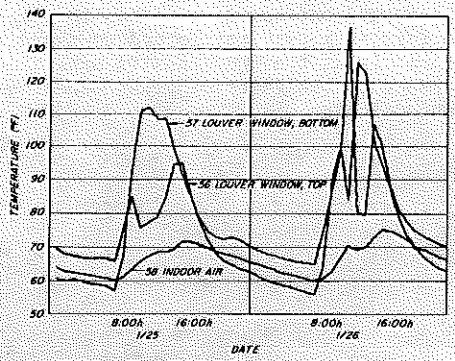

Figure 8. Temperature profiles for louver window of louver-window cabin. Irregulatities in louver-window temperature profiles show effects of cloudiness. Higher temperature peaks for Jan. 26 than for Jan. 25 suggest brighter sunlight. The integrated radiation level for Jan. 26, however, is only 4% higher than for Jan. 25 (Fig. 7)

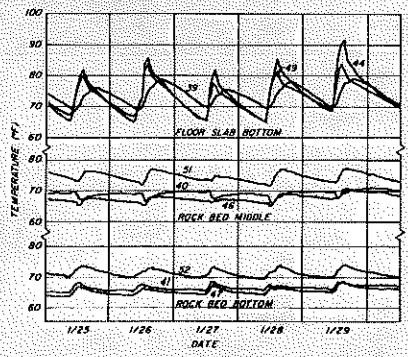

Figure 9. Temperature profiles for bottom of floor slab (location of points shown in Fig. 4) of louver-window cabin. Differences in temperature profiles between points 40, 46, and 51 are attributable to their relationship to air manifold layout.

--Temperature profiles for middle of rock bed: Differences in temperature profiles between points 40, 46, and 51 are attributable to differences in manifold placement and variations in airflow resistance through the rock bed

--Temperature profiles for bottom of rock bed

Discussion

R.H. McEntire, DAE Engineering, Logan, UT: Please clarify window construction.

G.E. Hans: Louver windows were composed on conventional double-glazed wood windows with 3/16-in. interior glass panel to form an airway for forced downward airflow over the venetian blind. The cavity was open to room air at the top, and its nighttime temperatures floated at room temperature level. The presence of the interior glass panel and the veletian blind, therefore, was disregarded in heat loss calculations.